Polarization-controlled multistage switch based on polarization-selective computer-generated holograms

Ashok V. Krishnamoorthy, Fang Xu, Joseph E. Ford, and Yeshayahu Fainman

We describe a polarization-controlled free-space optical multistage interconnection network based on polarization-selective computer-generated holograms: optical elements that are capable of imposing arbitrary, independent phase functions on horizontally and vertically polarized monochromatic light. We investigate the design of a novel nonblocking space-division photonic switch architecture. The multistage-switch architecture uses a fan-out stage, a single stage of 2×2 switching elements, and a fan-in stage. The architecture is compatible with several control strategies that use 1×2 and 2×2 polarization-controlled switches to route the input light beams. One application of the switch is in a passive optical network in which data is optically transmitted through the switch with a time-of-flight delay but without optical-to-electrical conversions at each stage. We have built and characterized a proof-of-principle 4×4 free-space switching network using three cascaded stages of arrayed birefringent computer-generated holographic elements. Data modulated at 20 MHz/channel were transmitted through the network to demonstrate transparent operation. © 1997 Optical Society of America

1. Introduction and Background

There is a growing need in the telecommunications and data-communications industry for a scalable switch that can provide high-throughput communication between a large number of input–output (I/O) ports. Recent advances in the area of fiber amplifiers has spurred interest in transparent optical networks, wherein communication between users is achieved without multiple conversions between the optical and electrical domains.[1] The implementation of 16×16 and larger switches in a number of optical technologies is currently being pursued. Moreover, polarization compensators have been developed for single-mode fibers to permit automatic and stable control of the polarization state of output optical signals.[2] One might thus envision a switching system that uses polarization-*dependent* optical switches. Because of its low-delay, high-throughput

characteristics, such a switch may also find applications in a tightly coupled multiprocessor networking system or a parallel-processor-to-memory interconnection. In fact, polarization switching has been widely proposed for use in the context of free-space optical multistage interconnection networks[3–7] for switch sizes up to 256×256.[8]

In this paper we describe a novel free-space polarization-controlled optical switch design and present the implementation of a 4×4 photonic switch. The potential advantages of this design include no bulky birefringent optical components, fewer optical surfaces resulting in lower insertion loss, no path-dependent attenuation nonuniformity, a reversible optical path, and greater flexibility in choosing the optical interconnect topology and the resulting switch architecture. The switching system is based on a unique polarization-selective optical element capable of acting with an arbitrary independent phase function on illumination with horizontally or vertically polarized monochromatic light. This element, known as a birefringent computer-generated hologram (BCGH), is composed of two birefringent substrates etched with surface-relief patterns and joined face to face.

In Section 2 we review the BCGH technology and discuss its application to the basic 2×2 switch. In Section 3 we describe a new, nonblocking multistage-switch architecture that is well suited to a photonic

A. V. Krishnamoorthy and J. E. Ford are with the Advanced Photonics Research Department, Bell Laboratories, Lucent Technologies, Holmdel, New Jersey 07733. F. Xu and Y. Fainman are with the Electrical and Computer Engineering Department, University of California, San Diego, La Jolla, California 92093-0407.
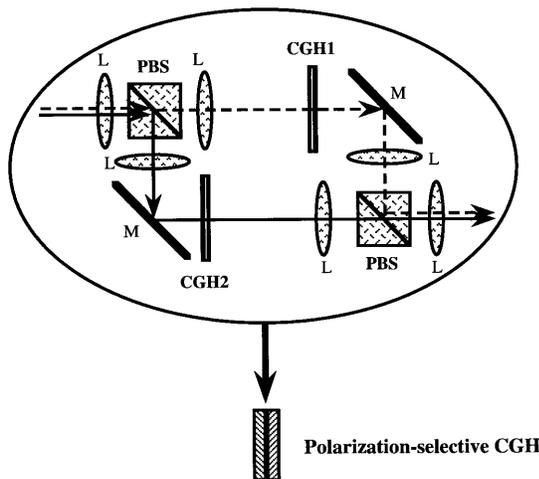
Fig. 1. Principle of operation of a polarization-selective hologram: The lenses represent two imaging stages of which the first imaging stage places one polarization on each Fourier-plane hologram and the second combines the outputs of the two polarizations. Here, 4-f imaging is required to transfer both the amplitude and phase of the incident wave front accurately. A BCGH combines the functionality of polarization beam splitters and associated interconnection optics in a single planar element.
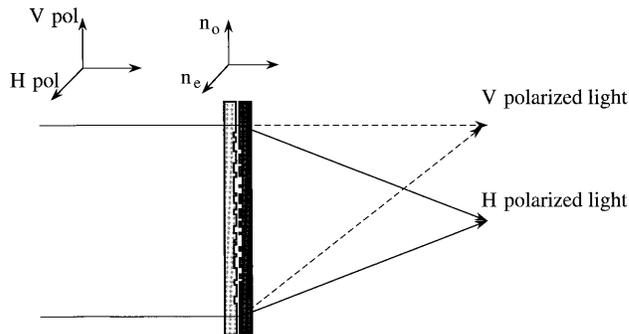

Fig. 2. Schematic diagram of the construction of BCGH's by the placement of two thin holographic elements face to face. At least one of the holograms is etched in an anisotropic medium (e.g., LiNO$_3$). H, horizontally; V, vertically; pol, polarized.

implementation with BCGH technology. In Section 3 we also present a discussion of system trade-offs and a comparison of the architectures with other well-known multistage-switch designs. In Section 4 we present the implementation and characterization of a 4 × 4 photonic BCGH switch. In Section 5 we provide a summary and conclusions.

2. Application of Polarization-Selective Computer-Generated-Hologram Technology to a 2 × 2 Switch

A. Birefringent Computer-Generated-Hologram Technology

Multistage interconnection networks (MIN's) using polarization switching can be built with polarizing beam splitters (PBS's) and other bulk optics. However, system costs and complexity limit the number of stages and therefore the network size. It is possible to simplify the system substantially and eliminate many of the optical alignments by replacement of the discrete optical components with polarization-selective planar holograms (Fig. 1). A PBS, imaging lenses (L), and two computer-generated holograms (CGH's) can be replaced by a single polarization-selective CGH that has a different phase profile for each of the two orthogonal linear polarizations (Fig. 2). Polarization-selective holograms have been fabricated with various techniques, including optical recording of dichromated gelatin,[9,10] organic media,[11] and photorefractive crystals,[12] as well as lithographic recording of polarization foil.[13] However, we are primarily interested in a particular type of polarization-selective hologram—the birefringent CGH, that is, a CGH fabricated in birefringent media.[14−17]

A conventional kinoform CGH is a two-dimensional (2-D) phase profile that transforms the input light (e.g., a plane wave) into the desired output (e.g., an array of points). The desired continuous phase profile is first computed and then reduced to a minimum of data by pixellation, truncation to modulo 2π, and quantization into discrete values. This data array is then used to fabricate the hologram. A BCGH is similar in function to a conventional phase-only kinoform CGH, except that a BCGH has a different phase profile for each of the two orthogonal linear polarizations that illuminate the hologram. One fabricates kinoform phase-only CGH's by etching a surface-relief profile into an isotropic glass substrate. In a BCGH, the surface-relief profile is etched into a birefringent substrate. The birefringent substrate provides different indices of refraction, depending on the input polarization, that are used to differentiate between horizontally and vertically polarized inputs. The information content of the two arbitrary phase functions is contained in two etched substrates, joined face to face so that both profiles effectively lie in the same optical plane (see Fig. 2). These two substrates can apply an arbitrary phase for the two orthogonal linear polarizations.

The operation of the BCGH can be explained by consideration of the case in which one substrate is birefringent and the other is isotropic and in which the polarization of the incident light is aligned either along or perpendicular to the optical axis of the birefringent substrate. A ray transmitted through the birefringent substrate will have a different phase delay for each polarization because the indices of refraction differ. At each pixel, the phase angle between the two polarizations and the absolute phase delay of the rays depends on the thickness, hence the etch depth, of the birefringent substrate. This etch depth is chosen to produce the desired final phase angle between the two polarizations. The ray then passes through the isotropic substrate, where light of either polarization is delayed by the same phase angle, again depending on the etch depth. This etch depth is chosen to bring one polarization to the desired phase angle. Because the relative delay between polarizations is unaffected by the isotropic substrate,

the phase angles of both polarizations are simultaneously brought to the final desired values. The result is an optical element that can have high diffraction efficiency and provide arbitrary functionality for each of the two orthogonal linear polarizations of the input light.

The BCGH element effectively splits the input light beams by polarization, acts independently on each beam by use of separate CGH's, and recombines–redirects the output beams (see Fig. 1). The process of computing, etching, and assembling a BCGH is described in greater detail elsewhere.[14–16] Methods of introducing artificial anisotropy in a transparent material by use of high-spatial-frequency, surface-relief nanostructures are also being investigated[18]; such investigation will ultimately permit BCGH elements to be fabricated on a single substrate.

B. Use of a Polarization-Selective Computer-Generated Hologram as an Optical 2 × 2 Switch

Two types of switch can be used for MIN's: 1×2 and 2×2 switches. A MIN can be made with $\vartheta(\log_2 N)$ stages of N, 1×2 switches per stage and $2N$ links between stages.[19] Switching is achieved by the choice of the output link each input takes. A switching MIN can also be constructed with $\vartheta(\log_2 N)$ stages of $N/2$, 2×2 switches per stage and N links between stages. Switching is achieved by the choice of the state of each 2×2 switch. This latter type of network is the one pursued in this paper.

As shown in Figs. 3(a) and 3(b), it is often convenient to build a 2×2 switch by use of 1×2 switches.[19–21] Figure 3(c) illustrates the allowed and disallowed states of the switch when 1×2 switches with passive combining are used to generate a 2×2 switch. The disallowed configurations of a 2×2 switch correspond to both inputs accessing the same output. For the case of a BCGH 2×2 switch, this situation would correspond to both polarizations having the same deflection angle at the output. If the inputs to the 2×2 switch have orthogonal polarizations, then the outputs will also have orthogonal polarizations when the axes of the electro-optic polarization modulator are aligned so as either to pass both polarizations without change or to rotate the polarizations of *both* beams by 90°. Hence, the disallowed configurations can be avoided if one ensures that the inputs to a 2×2 switch have orthogonal polarizations and if a 0° or 90° polarization-rotating switch is used.

A 2×2 polarization switch will thus require two BCGH planes and a polarization-rotator plane, as shown in Fig. 4. The two inputs are both directed into the first BCGH, which combines and focuses the two inputs into a polarization rotator (PR). After being combined, the two modulated beams propagate in the same direction through the PR; this step is essential to obtaining high-contrast modulation because polarization rotators are strongly angle sensitive. The PR sandwiched between the two BCGH elements controls the state of the 2×2 switch, i.e., either a crossover or straight-through connection. If

(a)

(b)

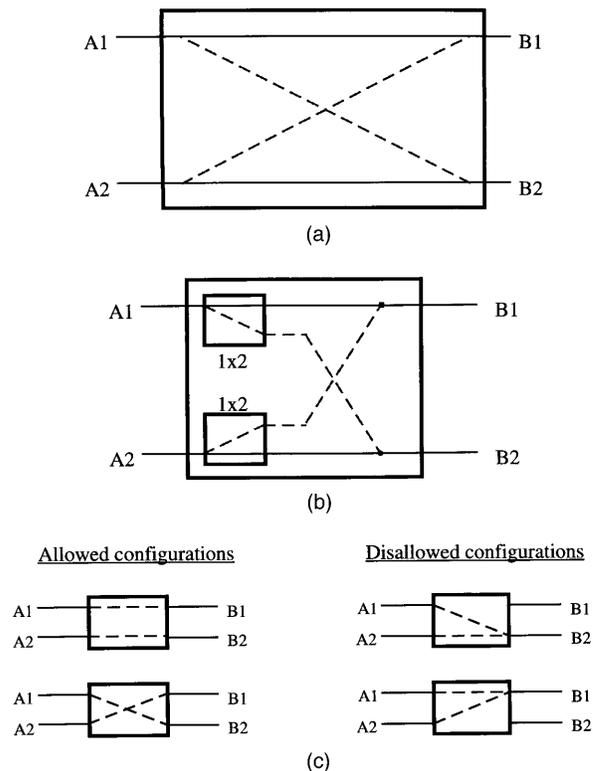Allowed configurations   Disallowed configurations

(c)

Fig. 3. Fabrication method and states of 2 × 2 switches: (a) A 2 × 2 switch either passes the inputs straight through or exchanges the inputs. (b) A 2 × 2 switch can be implemented by use of two 1 × 2 inputs with their respective outputs tied together. (c) Allowed and disallowed states. Disallowed states must be carefully avoided. In a BCGH implementation this is ensured by the requirement that the two inputs have orthogonal polarizations and by use of a 0° or 90° PR switch.

the PR is in the OFF state, the two beams propagate straight through, maintaining their original polarizations. When the PR is turned ON, the two beams exchange polarizations.

After transmission through (and possibly modulation by) the PR, the second BCGH element deflects the beams into two different directions, depending on their polarization states. Figure 4 shows the beam
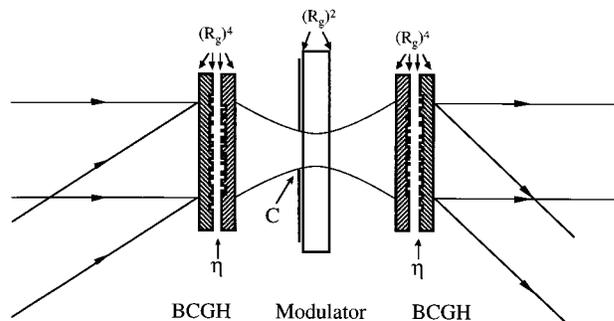

Fig. 4. Components of a 2 × 2 switch: two BCGH's and a polarization modulator. η is the switch efficiency, R is the transmittance, and C is the coupling efficiency associated with clipping losses, which are incurred when imaging a beam through a modulator aperture.

focused through a small aperture, which may or may not be necessary, depending on the modulator technology. Note that a BCGH switching element combines the functionality of a 2×2 switch and the associated holographic interconnection optics before and after the 2×2 switch. A 2×2 BCGH switch also has the same functionality for beams propagating through the optics in reverse, in principle making the network path reversible.

C. Insertion loss calculation for a 2×2 Polarization Switch

Optical loss in a BCGH switch is due to reflections from the dielectric surfaces and the diffraction efficiency of the holograms. To increase the diffraction efficiency of a BCGH hologram, and thus reduce the insertion loss (attenuation) of a BCGH-based switch, multilevel phase BCGH's are necessary. The theoretical diffraction efficiency of a CGH is proportional to the number of phase levels Φ used in its construction.[22] The efficiency of a BCGH η_{BCGH} is the product of the efficiencies of its two component holograms:

$$\eta_{\mathrm{BCGH}} = \mathrm{sinc}^2\!\left(\frac{1}{\Phi_a}\right)\mathrm{sinc}^2\!\left(\frac{1}{\Phi_b}\right). \qquad (1)$$

For instance, the use of four phase levels ($\Phi_a = \Phi_b = 4$) in each of the holographic elements results in an optimum BCGH diffraction efficiency of approximately 64%. Several four-level phase BCGH elements, each consisting of a 4×4 array of blazed gratings, were designed and fabricated for application to the MIN described below in Section 4. The grating periods were 40 μm, and the smallest feature size in the hologram was 10 μm. A diffraction efficiency of 26% and a polarization contrast ratio of 130:1 were measured for the four-level phase element. These values can be compared with a measured diffraction efficiency of 12% and a contrast ratio of approximately 50:1 with a binary phase element having the same feature size. By tilting the hologram to compensate for alignment errors, Xu $et\ al.$[16] have achieved best-case results for a four-level phase hologram of a 60% diffraction efficiency and a 160:1 contrast.

Surface-reflection losses at the BCGH substrate R_g and the modulator substrate R_m contribute to the switch loss. A clipping loss C occurs when the beams are focused through an aperture at the modulator. The total switch efficiency is then

$$\eta_{\mathrm{switch}} = \eta_{\mathrm{BCGH}}^{2}R_g{}^{8}R_m{}^{2}C. \qquad (2)$$

If we assume that each optical surface is antireflection coated with a single dielectric layer (to permit the maximum range of input angles) and that 16-level phase holograms are used, then these constants can be estimated to be $\eta = 98.4\%$, $R_g = R_m = 99\%$, and $C = 98.6\%$. The total switch efficiency is then 86.3%, producing an insertion loss of 10 $\log_{10}(\eta_{\mathrm{switch}}) = -0.638$ dB. The calculations presented here represent the switch performance of a

transmission device. Note that BCGH components may also be used in conjunction with smart-pixel technology. Depending on the particular device technology, this combination can introduce other surfaces (e.g., a common substrate that holds the circuit and the modulator materials).

If the polarization rotation were exactly $\pi/2$ and the BCGH's distinguished completely between the two polarizations, the cross talk would be zero and the signal-to-noise ratio (SNR) of a 2×2 switch would be infinite. In practice, one can define the cross talk coming from one switch to be δ_c and the maximum number of switches in one path to be S. Then the SNR of the entire network is given by

$$\mathrm{SNR}_{\mathrm{network}} = \log_{10}(1/\delta_c) - \log_{10}S. \qquad (3)$$

Note that δ_c is a critical factor that will determine the choice of architecture and maximum network size. In this paper we consider two examples: $\delta_c = 0.1\%$ and $\delta_c = 1\%$. These two cases are typical of currently achievable technology for bulk and pixellated BCGH switching elements.

3. Architecture of the Birefringent Computer-Generated Hologram Multistage Switch

A. Switch Architecture

The Stretch network is a class of self-routing MIN's that provides a continuous performance–cost trade-off between two of its extreme forms: the fully connected space-division switch (or crossbar switch) and the Banyan multistage network. Stretch networks utilize a destination-tag-based routing algorithm; that is, for each input channel, the necessary I/O path through the network can be determined on a stage-by-stage basis solely from the specified destination of the input packet. Stretch networks can be designed to achieve a low delay and arbitrarily low blocking probabilities for various traffic patterns without using internal buffers in the switching fabric. A common feature of all Stretch networks is that each stage in the multistage switching network uses a simple perfect-shuffle interconnection or any of the topologically equivalent connection patterns.[23] In this paper we are concerned with a specific nonblocking Stretch network with N I/O channels and k-shuffle interconnection between stages. The broader class of Stretch networks is described in more detail elsewhere.[24]

An example of the switch architecture for $N = 8$ channels is presented in Fig. 5(a). In this network, the fan-out (splitting) stages [Fig. 5(b)] permit partial contention-free routing of the first $\log_2(N-1)$ bits of the destination address for each of the N inputs; the switching stage provides the routing on the last bit of the destination address, and the fan-in (combining) stages [Fig. 5(c)] concentrate the outgoing data. The fan-out and fan-in stages provide contention-free demultiplexing and multiplexing, respectively, of each input signal. The fan-out stage is connected to the switching stage by use of a two-shuffle connection
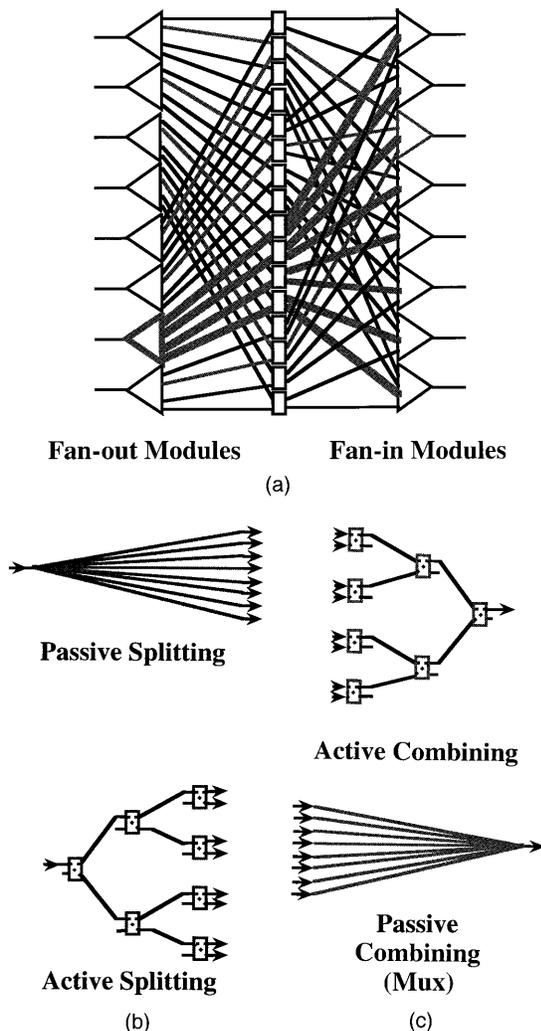
Fan-out Modules **Fan-in Modules**

(a)

Passive Splitting

Active Combining

Active Splitting

Passive Combining (Mux)

(b) (c)

Fig. 5. (a) Stretch switch with eight inputs–outputs, a fan-out of 4, and one stage of 2×2 switches. The switch is nonblocking, and the first-order cross talk of the network is equal to the cross talk of a single switch. All lines represent point-to-point connections. (b) Fan-out modules may either be passive or active. (c) Fan-in, similarly to fan-out, may be active, passive with optical fan-in, or implemented with separate detectors and electrical multiplexing (Mux).

pattern, and the switching stage is connected to the fan-in stage by use of a $(N/2)$-shuffle connection pattern. Notice that the fan-out for each input is $N/2$, which is half the fan-out for a fully connected switch. A single stage of 2×2 switches is used in the center of the switching fabric. An important consequence is that the switch is strictly nonblocking, with a unique constant-length path from each input port to each output port. This can be verified visually from Fig. 5(a) and is proved in Ref. 25. The highlighted connections in Fig. 5(a) show the path from a specific input to each of the output ports.

This nonblocking architecture is well suited for parallel optical implementation because it uses a single stage of $N^2/2$, 2×2 switching elements and because the destination-tag-routing property of the multistage switch results in a simple path-hunt al-

gorithm that can readily be accomplished in parallel if required. The structure of this switch is, in principle, similar to the extended generalized shuffle network described in Ref. 20, except that the Stretch network has an exact multiple of log N logical stages (including the fan-out modules) between the input and output ports, thereby ensuring a self-routing structure, hence a simple routing algorithm, that may be applied to each channel independently of the others.

The implementation of the fan-out and fan-in stages in an optical Stretch network is critical to the network's performance. The fan-out stage may be passive (i.e., optical broadcast) [passive splitting (PS)], which results in a maximum $2/N$ power efficiency, or it can be active [active splitting (AS)] i.e., built by use of a tree-based architecture with $N/2$ additional 1×2 switches per fan-out module.[26] Similarly the fan-in stage can be active (built with 2×1 switches) [active combining (AC)], passive with optical fan-in [passive combining (PC)], or can use $N/2$ separate receivers per output module with electronic multiplexing. For the active tree-based fan-out and fan-in modules, the control lines in a stage are typically tied together for convenience; hence each module will require $\log_2(N - 1)$ control lines to control $N/2$ switches.

When AS is used, each fan-out stage consumes the first $\log_2(N - 1)$ bits of the destination address of the corresponding inputs, and the 2×2 switching stage consumes the last bits to achieve a unique output address for each of the N inputs. In this mode, the network can be self-routing. The nonblocking network structure ensures that no permutation can result in network blocking or a disallowed switch state. If PS and AC are used, then the network controller must work in reverse by use of sender-tag routing, in which the fan-in unit is set according to the last $\log_2(N - 1)$ bits of the sender address and the 2×2 switching stage is set according to the first bit of the sender tag. In addition, the top half of the inputs must be polarized orthogonally to the lower half of the inputs to ensure proper operation of the 2×2 BCGH switches. When active fan-out and active fan-in modules are present, both destination-tag and sender-tag algorithms are used. In all cases, the path-hunt algorithm and the switch-setting process may be performed independently and in parallel for each of the N channels. This property enables the path hunt to be performed in $O(\log N)$ time steps. Note that special care must be taken to ensure that the inputs to a 2×2 switch in the switching stage have orthogonal polarizations. When PS is used together with a shuffle interconnection topology, then one method of ensuring this is to polarize the top half of the inputs orthogonal to the lower half. If AS is used with an optical shuffle, then the polarizations of subsequent outputs alternate, and the polarizations of the lower half of the inputs mirror the upper half.
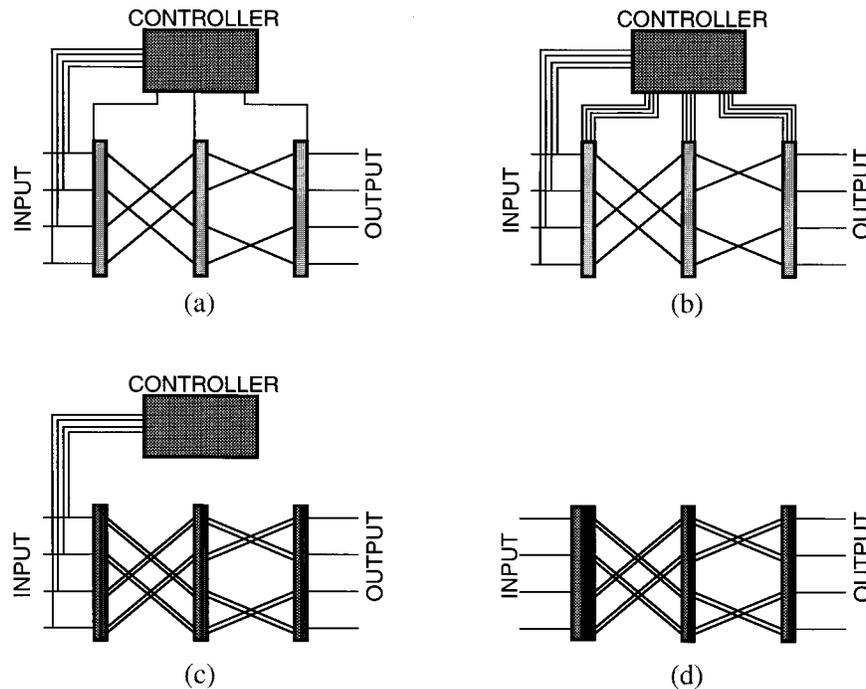
Fig. 6. Possible control algorithms for BCGH-based MIN's: (a) centralized control with global switching, (b) centralized control with direct injection, (c) centralized control with packet headers, and (d) distributed control with self-routing headers.

B. Control Algorithms

In a BCGH-based Stretch network, the switch can operate in a transparent circuit-switched mode and can be either locally or globally routed. The setup and reconfiguration times depend on the specific polarization-modulator technology, but after the network state is set the data-transmission rate is limited only by signal attenuation, cross talk, and factors external to the multistage switch, i.e., the transmitter and receiver responses. Communication involves three phases: (i) circuit establishment, in which end-to-end circuits are set up before transmission begins; (ii) data transmission, in which the data-modulation rate is decoupled from the reconfiguration of the network; and (iii) circuit disconnect. The switch described in this paper is of the space-division switching type, with the added possibility that the inputs to the network may be time-division or wavelength-division multiplexed (e.g., from an optical-fiber bundle).

A key concern is the control of the network's switching states. Several distinct types of control algorithms can be defined: centralized control with global switching, centralized control with direct injection, centralized control with packet headers, and distributed control with self-routing packet headers.[27] Figures 6(a)–6(d) show each approach schematically. In centralized control with global switching, the switches in each layer of the network are linked and can only switch as a unit. The number of control lines is greatly reduced, but only a single arbitrary interconnection of one input to one output can be made at a time. This functionality is useful in the fan-out (fan-in) modules for which a single input (output) must be steered to a select channel, so that the control lines of the 1×2 (2×1) switches in a column may be tied together. This reduction in control lines potentially increases second-order cross talk through the network.

The second method is to use centralized control with direct injection. In this scheme the routing algorithm is calculated at a central controller that determines switch settings and accesses the switching elements sequentially or in a semiparallel fashion. For controlling large networks it becomes essential to have an architecture, such as the Stretch network, that allows path hunts to be performed in parallel.

Another approach is to use centralized control with packet headers. The routing algorithm is performed at a centralized controller, but the process of setting the individual switches of the MIN is implemented by use of packet headers that propagate through the network. This approach can be achieved by use of ≤ 30 transistors per switch and can be achieved by use of a BCGH coupled with smart-pixel technology. The routing information must still be distributed to the first-stage array, but not to the arrays at each layer of the network. For BCGH-based networks using this form of control, virtual circuit switching is achieved by the specification of a dedicated time interval for the packet headers with control information to propagate through the network and set up the required data paths. As soon as the switches have been set, passive transmission (no detection and re-broadcast) at high data rates is possible. For transparent operation, control may optionally be at a

distinct wavelength or on a separate path. The main advantage of this method is a reduced controller pin-out (a factor of at least $\log_2 N$ fewer than direct injection). However, this approach requires synchronous network operation and a technology that can provide some intelligence at each pixel location.

A fourth approach is to use distributed control with self-routing packet headers. Here, no central controller is needed. This algorithm is typically associated with fast packet switching. A smart-pixel implementation will require 50–75 transistors per 1×2 switch.[21] This approach uses the same smart-pixel hardware and interconnection topology as the centralized approach with packet headers. These packet-header control approaches are relevant for only BCGH networks that use active fan-out or active fan-in (or both).

C. Comparison of Nonblocking Networks

Two key performance metrics for a passive multistage photonic switch architecture are its optical attenuation and its SNR or cross talk. These in turn are related to the amount of optical fan-out per input, the number of stages in the multistage-switching network, and the number of switches an input signal must traverse to reach its intended output (path length). In the following we analyze the performance of the nonblocking Stretch network in terms of its cross talk and attenuation relative to some well-known nonblocking MIN architectures that are suitable for implementation with the 2×2 BCGH switches. These include the crossbar, N-stage planar,[28] Benes,[29] dilated Benes,[30] and Batcher–Banyan networks.[31] A more detailed discussion of these switching-network architectures can be found in Refs. 28–32.

In terms of nonblocking architectures for photonic switching, the most well-known switch architecture is the crossbar. The crossbar (or full space-division switch) is a strictly nonblocking architecture with N^2 switches and a worst-case path length of $2N - 1$. In a crossbar, the path length and the signal skew depend on the specific interconnection path. The N-stage planar network is a rearrangeable nonblocking architecture requiring N stages with $N/2$ switching elements per stage. It evolved from the crossbar, providing fewer switches and a planar (no crossover) architecture by use of only the nearest-neighbor interconnection and equal path lengths. The total number of switches is $N(N - 1)/2$, and the maximum path length is N.

In terms of nonblocking multistage architectures that require significantly fewer 2×2 switches, a widely studied architecture is the Benes network. The rearrangeable nonblocking Benes network consists of two $\log_2 N$ networks placed end to end. The network has $2 \log_2 N - 1$ stages, which is the theoretical minimum number of stages required for rearrangeable nonblocking operation. This network provides an equal path length, low latency, and low switch count at the expense of a more complicated routing overhead.

The dilated Benes architecture was a modification of the Benes network designed to remove effects of cross talk that plague architectures with a $\log N$ or greater depth. This is a Benes network that has been doubled in width while the initial number of inputs and outputs has been maintained. Dilated Benes networks thus have $2 \log_2 N$ stages and N switches per stage. The network has the unique advantage that no switching element carries more than one active signal. Hence, first-order cross talk is eliminated. Optical cross talk from another channel can be mixed with an active signal only by its passing through two nominally OFF switches. When this second-order cross talk is low, the network can achieve a large SNR. Finally, the Batcher–Banyon network is a self-routing network consisting of a sorting network followed by a routing network. The total number of stages is equal to $(1/2)\log_2^2 N + (3/2)\log_2 N$.

Table 1 contains a summary of the attenuation, SNR, number of stages, and total number of switches for each of the nonblocking architectures described above versus the network size N. Table 2 similarly shows the scaling of the SNR, attenuation, and switch count of the various configurations of the Stretch network. The results depend strongly on the type of fan-out and fan-in modules used. For instance, the number of stages in a Stretch network depends on the design of the fan-out (splitting) and fan-in (combining) stages. It is $\log N$ if either the splitting or the combining is active (AS/PC or PS/AC), $2 \log_2 N - 1$ if both the splitting and combining stages are active (AS/AC); or 1 if no active switching is used (PS/PC with separate receivers).

As a result of SNR degradation, optical fan-in to a common detector is feasible only for smaller networks. The first-order cross-talk isolation of the AS/AC Stretch network is equal to the cross-talk isolation of a single switch, independent of network size. The second-order cross talk is much smaller in magnitude than the first-order cross talk and can be neglected. The attenuation and the SNR for $\beta_c = 30$, 20 dB, respectively, are graphed in Figs. 7–9. The corresponding performance of several Stretch networks is shown for comparison. The dotted cutoff lines show the maximum achievable sizes of each architecture, assuming a maximum acceptable attenuation to be 30 db (99.9%) and the minimum SNR to be 11 dB (corresponding to a bit error rate of 10^{-9}).[32] It should be noted that the SNR can be increased at the price of increased attenuation. For example, if the fan-out in the Stretch network were increased from $N/2$ to N, there would be no first-order cross talk and the SNR could be doubled. In this case second-order cross talk must be accounted for. The resulting network would be identical to a full space-division switch,[28] and it would have increased attenuation and would also require more switching elements (Table 2).

It is evident that nonblocking networks, such as crossbars or N-stage planar networks, are not well suited to large-scale implementation with a BCGH.

Table 1. Performance Scaling for Several Well-Known Photonic Switch Architectures in Terms of the Network Size *N*

Architecture[a] (N inputs/ N outputs)	Attenuation[b] (dB)	SNR[c] (dB)	Number of Logical Switching Stages	Number of 2×2 Switches[d]
Crossbar (nonblocking)	$(2N - 1)\alpha_s$	$\beta_s - 10 \log_{10}(N - 1)$	N	N^2
N-stage planar (nonblocking)	$N\alpha_s$	$\beta_s - 10 \log_{10} N$	N	$N(N - 1)/2$
Batcher-Banyon (nonblocking)	$[1/2 \log_2 N(\log_2 N + 1) + \log_2 N]\alpha_s$	$\beta_s - 10 \log_{10}$(number of stages)	$1/2 \log_2 N(\log_2 N + 1) + \log_2 N$	$N/2$(number of switches)
Benes (rearrangeable, nonblocking)	$(2 \log_2 N - 1)\alpha_s$	$\beta_s - 10 \log_{10}(2 \log_2 N - 1)$	$2 \log_2 N - 1$	$N/2(2 \log_2 N - 1)$
Dilated Benes (rearrangeable, nonblocking)[e]	$2(\log_2 N)\alpha_s$	$2\beta_s - 10 \log_{10}(2 \log_2 N - 1)$	$2 \log_2 N$	$2N \log_2 N$

[a]The architecture was circuit switched.
[b]For the worst-case optical path loss. α_s is the insertion loss per switch, in decibels.
[c]For the worst-case SNR. β_s is the cross-talk isolation per switch, in decibels.
[d]In the entire network.
[e]The SNR in this case is due to second-order cross talk.

In terms of attenuation limits, the Batcher–Banyan MIN scales up to 256 I/O ports. The Benes, dilated Benes, and Stretch networks with AS scale well beyond $N = 1000$, making them good choices (Fig. 7). Power losses that are due to fan-out limit Stretch networks with PS to fewer than 512 I/O ports. When the cross-talk isolation of a switch β_s equals 30 db, all these networks perform well in terms of SNR. However, when β_s is lowered to 20 db, the cross talk from the switches along the routing paths severely limits the scalability of Benes networks, and to a lesser extent the Stretch networks with PS. In this case, either a dilated Benes network or a Stretch network with AS must be used to counter the deleterious effects of cross talk (Figs. 8 and 9).

The conclusion is that the nonblocking Stretch network with AC is a suitable candidate for a BCGH-based switch implementation and has good potential for extension to large networks. The main advantages of the Stretch network over other suitable multistage networks, such as the dilated Benes, are its nonblocking operation without the need for rearrangement and its simple, parallel path-hunt capability. Among the nonblocking networks, it has the

Table 2. Performance Scaling for Various Configurations of the Stretch Network versus the Network Size *N*[a]

Architecture[b] (N Inputs/N Outputs)	Attenuation[c] (dB)	SNR[d] (dB)	Number of Logical Switching Stages	Switches Number[e]	Switches Type
Stretch AS/AC tied control lines	$(2 \text{Log}_2 N - 1)\alpha_s$	β_s	$2 \log_2 N - 1$	$N(N - 2) + (N^2/4)$	1×2 2×2
Stretch AS/AC separate control lines	$(2 \log_2 N - 1)\alpha_s$	β_s	$2 \log_2 N - 1$	$N(N - 2) + (N^2/4)$	1×2 2×2
Stretch PS/AC tied control lines	$(\log_2 N)\alpha_s + 3(\log_2 N - 1)$	$\beta_s - 10 \log_{10}(\log_2 N - 1)$	$\log_2 N$	$N(N/2 - 1) + (N^2/4)$	1×2 2×2
Stretch AS/PC tied control lines; fan-in to receivers	$(\log_2 N)\alpha_s$	$\beta_s - 10 \, log_{10}(N/2)$	$\log_2 N$	$N(N/2 - 1) + (N^2/4)$	1×2 2×2
Stretch PS/PC separate receivers	$\alpha_s + 3(\log_2 N - 1)$	β_s	1	$(N^2/4)$	2×2
Full space-division switch AS/AC fan-out equals N	$(2 \log_2 N)\alpha_s$	$2\beta_s - 10 \log_{10}(\log_2 N)$ (second-order cross talk)	$2 \log_2 N$	$2N(N - 1)$	1×2

[a]Either AS or PS may be used in the fan-out module. For small networks, the fan-in modules may use PC with either optical fan-in or separate receivers. For large networks, the fan-in modules should use AC. The control signals in a stage of an active splitting (fan-out) or an active combining (fan-in) module can be tied together to reduce the number of separate control lines.
[b]The architecture is circuit switched.
[c]For the worst-case optical path loss. α_s is the insertion loss per switch, in decibels.
[d]For the worst-case SNR. β_s is the cross-talk isolation per switch, in decibels. SNR is limited by first-order cross talk unless otherwise noted.
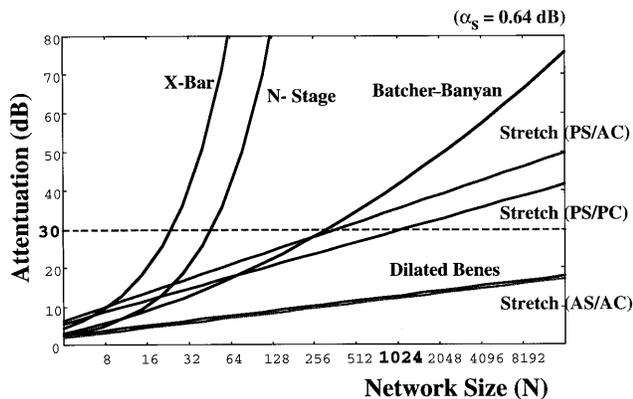[e]Number in the entire network.

Fig. 7. Network attenuation α_s (in decibels) versus the number of input ports N for BCGH-based MIN's with the assumption of a 2×2 switch insertion loss of 0.64 dB. X-Bar, crossbar.
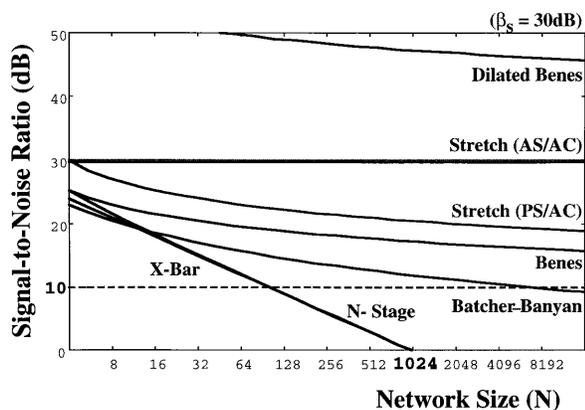

Fig. 9. Network SNR β_s (in decibels) versus the number of input ports N for BCGH-based MIN's with the assumption of a 2×2 switch SNR of 20 dB. X-Bar, crossbar.
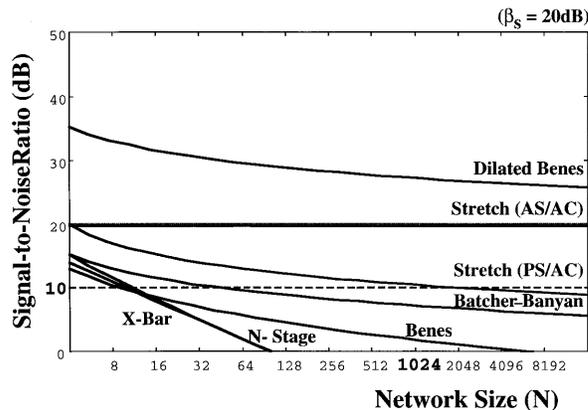
fewest number of optical stages. This reduces the network delay and control complexity. The penalties are its increased attenuation when PS is used and its larger number of switches when AS is used. For switching networks with less than 512 I/O ports, PS can be used; for larger networks, AS may become necessary. Technological limits to the BCGH Stretch network with AS arise primarily from array-size limits of the pixellated polarization modulator ($N^2/4$ pixels needed) and the maximum size of the birefringent hologram.

4. 4 × 4 Switch Demonstration

BCGH components have previously been evaluated for a 1×2 switch[15] and a 2×2 switch.[16,33] Here we describe the first multistage switching network demonstration based on cascaded arrays of polarization-selective holographic components. We have designed and implemented a three-stage, 4×4 BCGH optical multistage switch that can be scaled to larger sizes. The 4×4 BCGH–Stretch network used centralized control with global switching for the fan-out module and centralized control with direct injection for the 2×2 switching stage. Figure 10

Fig. 8. SNR β_s (in decibels) versus the number of input ports N for BCGH-based MIN's with the assumption of a 2×2 switch SNR of 30 db. X-Bar, crossbar.

shows a schematic diagram of the network architecture, and Fig. 11 shows a schematic diagram of the experimental setup. The switch consists of three cascaded BCGH switch arrays, two PR's, and four photodetectors. The fan-out (splitting) stage of the network is an array of 1×2 switches, and it consists of BCGH1 and a PR. The second stage of the network is an array of 2×2 switches. It is constructed by use of BCGH2 and BCGH3 together with a PR. PC of the beams occurs on four photodetectors (one for each output channel) that serve as the output stage of the network. In general, passive optical fan-in is feasible only for smaller networks (see Table 2). The SNR can be increased by use of a stage of active fan-in modules. Note that the 4×4 implementation used a butterflytype interconnect, instead of the shuffle. This permitted smaller deflection angles and allowed a single type of element to be used when the network was folded into two dimensions.

The three BCGH arrays were identical four-level phase, polarization-selective diffractive elements, as shown schematically in Fig. 12. The BCGH switching elements were fabricated by use of standard microfabrication technologies: electron-beam lithography was used to define the mask patterns; optical lithography was employed to transfer the pattern onto the Y-cut lithium niobate substrate; the surface-relief profile was obtained through the use of ion-beam etching. Each BCGH array consisted of a 4×4 array of pixels, where each pixel corresponds to a 1×2 switch. The dimensions of each pixel were approximately 4 mm $\times$ 4 mm, so the overall element had an active area of 1.6 cm $\times$ 1.6 cm (Fig. 13).

Each of the 16 switches in an array was a diffractive polarization beam splitter designed to propagate vertically polarized light (solid lines in Fig. 11) straight and to deflect horizontally polarized light (dashed lines) at an angle. The grating period was 40 μm, and the operating wavelength was 514.5 nm. These parameters set the optimum distance between the two BCGH arrays to be approximately 320 mm. Figure 14 shows a photograph of the system that
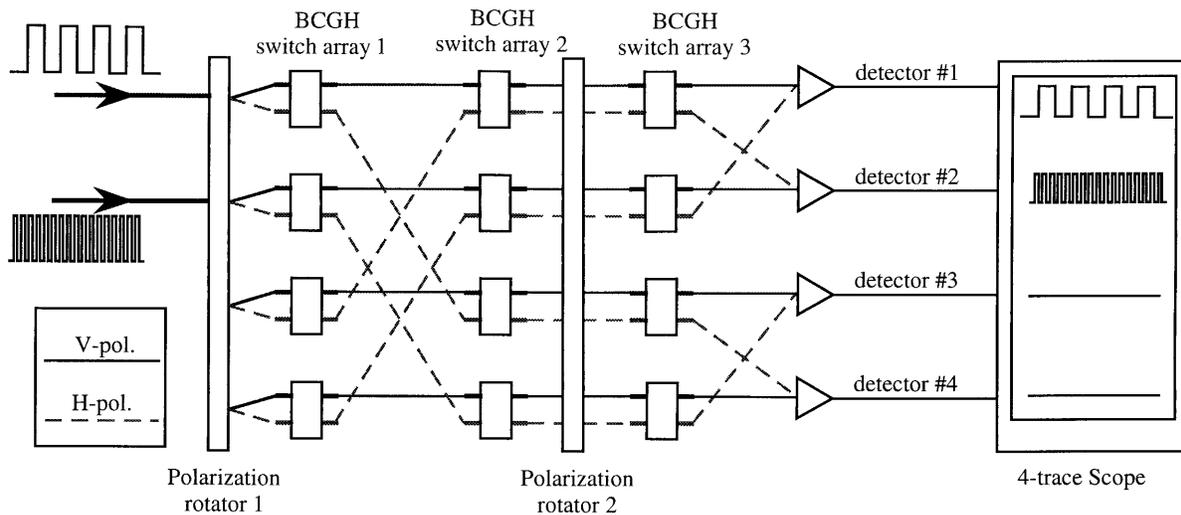
Fig. 10. Schematic diagram of a 4 × 4 BCGH Stretch switch. The demonstration system in this study employed a two-dimensional folded version of the optical 2-shuffle interconnection. Scope, oscilloscope; V-pol., vertically polarized; H-pol., horizontally polarized.
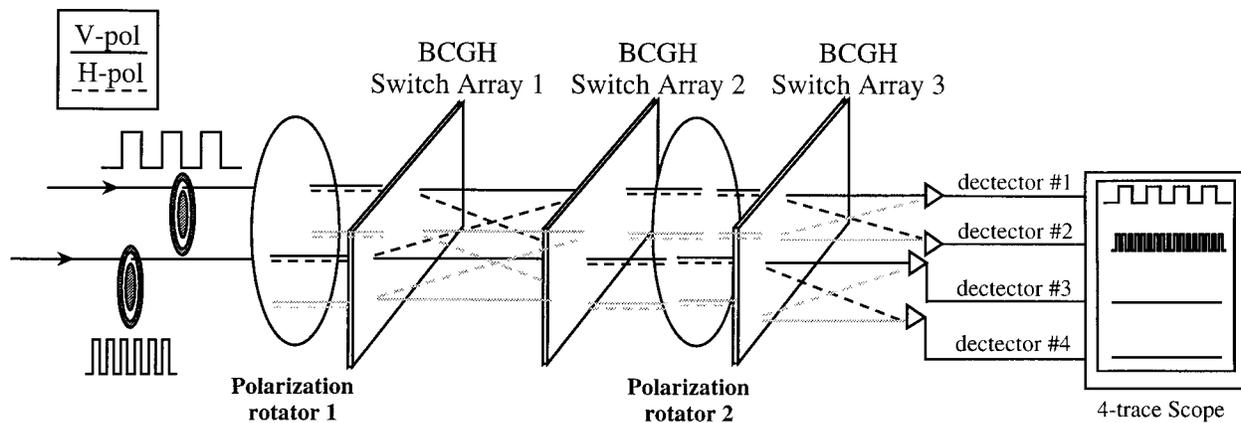

Fig. 11. Diagram of the optical system for the 4 × 4 switch implementation for tracing two input paths. In the implementation, the network was folded into a two-dimensional array with equal spacing in the horizontal and vertical directions. Scope, oscilloscope; V-pol., vertically polarized; H-pol., horizontally polarized.

displays the cascaded BCGH arrays. A collimated laser beam was used in the experiment, without any relay imaging optics between the BCGH holograms. The measured diffraction efficiencies of the BCGH

Fig. 12. Schematic cross section of the BCGH used for the MIN studied here. The BCGH was fabricated in LiNbO$_3$. The substrate thickness was 1 mm, and the operating wavelength was 514.5 mm.

holograms were approximately 26%, with peak polarization contrast ratios of 130:1.

Two broadband manual PR's and two electrically controlled liquid-crystal polarization rotators (LCPR's) were used to characterize the switching network and to demonstrate the reconfiguration of the network, respectively. The contrast ratio of the PR's (Newport, Model PR-550) and the Hughes LCPR's were 1000:1 (30 dB) and 4:1 (6 dB), respectively. A beam from an Ar$^+$ laser was split into two paths, and two mechanical beam choppers modulated at 300 and 900 Hz were used to label the two input beams. To characterize the performance of the network, the SNR was measured at each output of the network by the intensity ratio between the ON state (one of the two input signals is routed to this output node) and the OFF state (both inputs are routed to other output nodes). The worst-case SNR at the output was measured to be 10:1 (10 dB) when both PR's were manual; the best-case SNR was 20:1 (13 dB). During normal
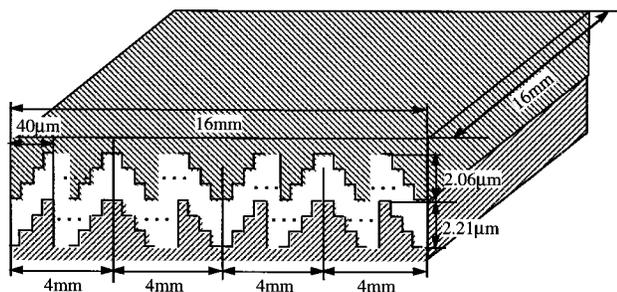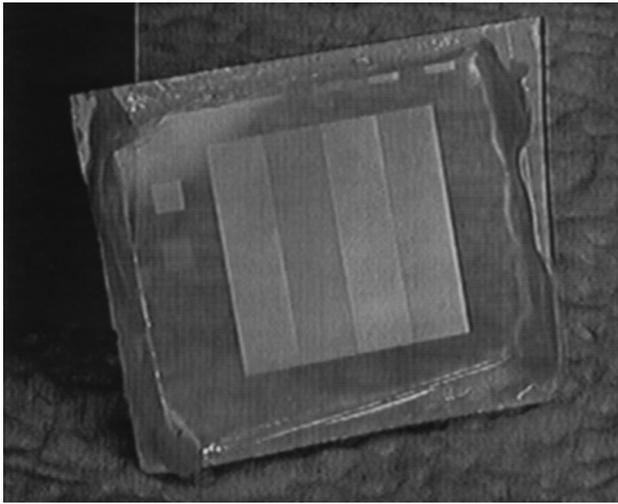
Fig. 13. Photograph of the 4 × 4 BCGH element array. The dimensions of the array are 16 mm × 16 mm.

network operation, LCPR's were used to provide electrically controlled reconfiguration. The 4 × 4 switch was tested with one and two active inputs. Figure 15 demonstrates one active input to the 4 × 4 switch being switched (reconfigured) between the four outputs. Figure 16 shows the output data with each input beam being switched between two corresponding outputs of the network. In both cases, the worst-case SNR was approximately 4:1, limited by the contrast ratio of the LCPR's.

The reconfiguration speed of the network was also limited by the temporal response of the PR's. The LCPR was operated at a maximum reconfiguration rate of approximately 1 KHz. Using PLZT (lead lanthanum zirconate titanate) or multiple-quantum-well PR's may make reconfiguration as fast as 10–100 MHz possible. Once these PR's were set at a specific configuration, the data rate was limited by

the frequency responses of the transmitters and receivers, because no signal regeneration was used inside the multistage switch. To demonstrate this, we used an acousto-optic modulator modulated at 20 MHz by a pseudorandom non-return-to-zero data generator to modulate one of the input signals. The eye diagram obtained at one of the outputs of the three-stage multistage interconnection network is shown in Fig. 17. Table 3 lists the performance values required of a 2 × 2 BCGH switch for large switches ($N \geq 1024$) and the best experimental results obtained to date. Note that the increased cross talk of approximately 3 dB for the experimental 4 × 4 Stretch switch versus that of the 2 × 2 switch is consistent with the predicted values from Table 2 (AS/PC).

5. Summary

This paper describes the design and implementation of a nonblocking space-division three-dimensional photonic multistage network architecture that uses 2 × 2 BCGH polarization-selective switches to switch and route the light at each node. The switch architecture uses a fan-out stage, a single stage of 2 × 2 switches, and a fan-in stage. This architecture is well suited for parallel optical implementation in that (a) it is nonblocking; (b) it enables fast, parallel path hunting with low latency communication; (c) it uses simple 2-shuffle and $N/2$-shuffle connection patterns (or their equivalents); (d) it uses one stage of $N^2/2$, 2 × 2 switching elements; and (e) it reduces the effects of first- and second-order cross talk. The fan-out stage may be passive (i.e., simple optical broadcasting), which results in a $2/N$ power efficiency, or can incorporate N fan-out modules (one per input port), where each fan-out module uses a tree-based architecture with $N - 1$, 1×2 switches. Similarly, the fan-in stage can either be active or can use $N/2$ separate detectors per fan-in module. The re-
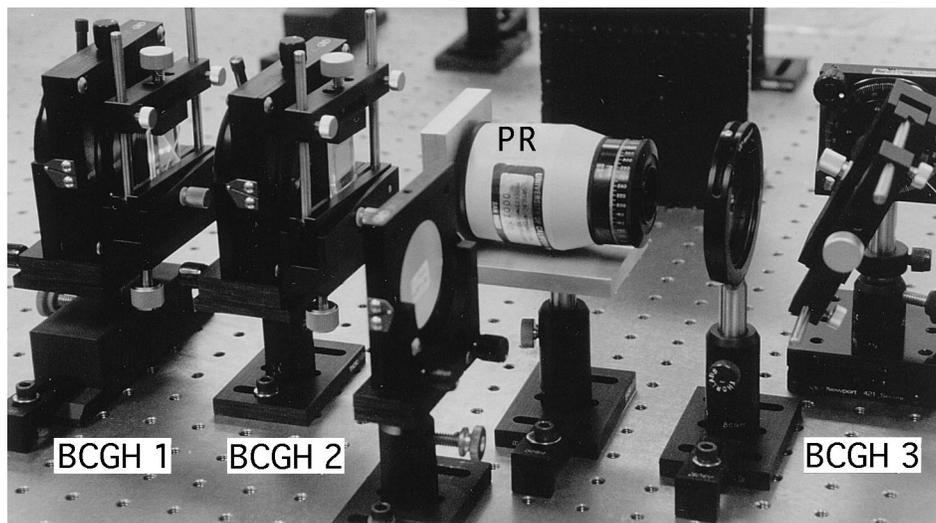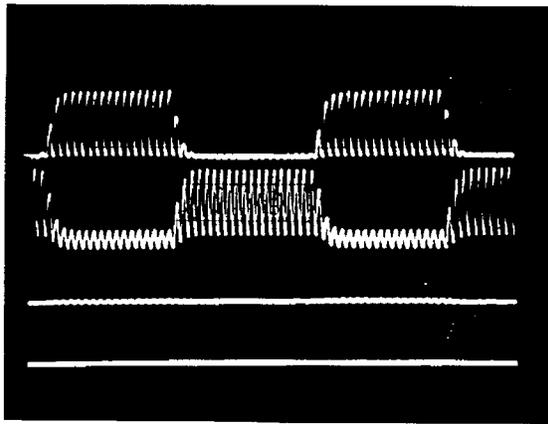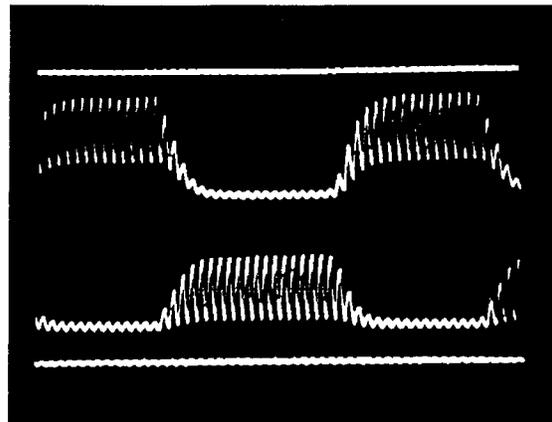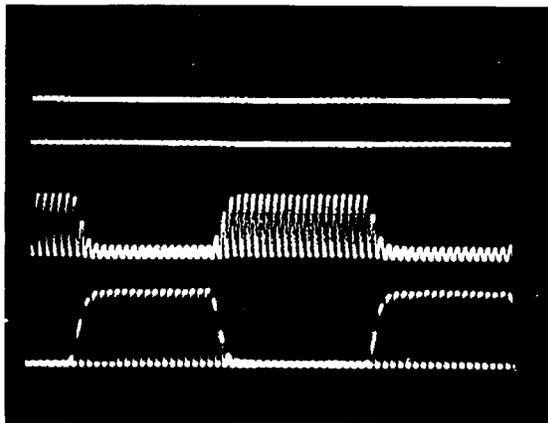

Fig. 14. Photograph of three cascaded BCGH arrays that formed the core of the demonstration free-space switch. The manual PR was used to characterize the network and was replaced by an electrically controlled LCPR for fast reconfiguration.
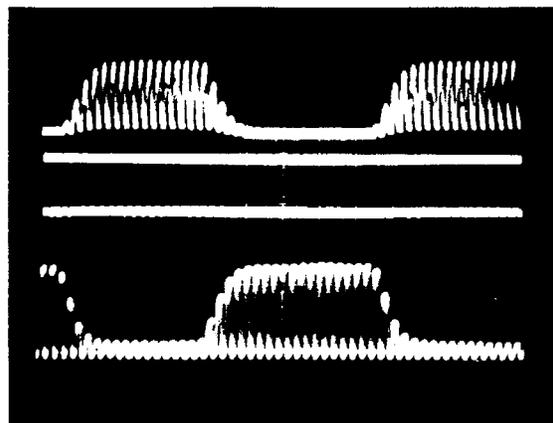
(a)

(b)

(c)

(d)

Fig. 15. Four-trace oscilloscope photographs showing the outputs of the 4 × 4 switch. An input to the 4 × 4 switch is being switched (reconfigured) between (a) outputs 1 and 2, (b) outputs 2 and 3, (c) outputs 3 and 4, and (d) outputs 1 and 4. Network cross talk was limited by the 4:1 contrast ratio of the polarization rotator. A SNR of 13 db was measured with manual PR's. The horizontal sweep rate is 10 ms/division.
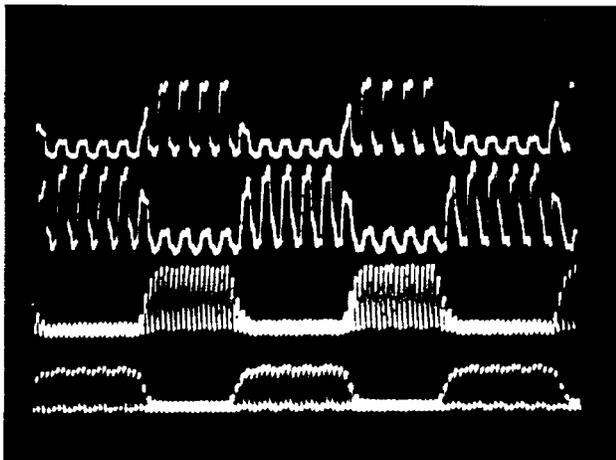

Fig. 16. Four-trace oscilloscope photographs showing two active inputs to the 4 × 4 switch being simultaneously switched between two outputs of the network. The horizontal sweep rate is 10 ms/division.

sulting photonic switch is circuit switched and can be either locally or externally controlled. The control choice will drive the required light-modulator technology and required pixel complexity. Network setup and reconfiguration times depend on the specific polarization-modulator technology, but after the polarization switches are set, the switching network is transparent, and the data-transmission rate is limited by the source and receiver response.

A small-scale network was demonstrated in an experimental 4 × 4 BCGH switch. The use of a high-performance pixellated polarization-modulator array, together with ongoing research on improving the performance of the BCGH elements, could make such a switch (with $N \geq 32$ ports) a useful candidate for high-speed optical networks, as well as for large-scale optical multiprocessor interconnection networks.
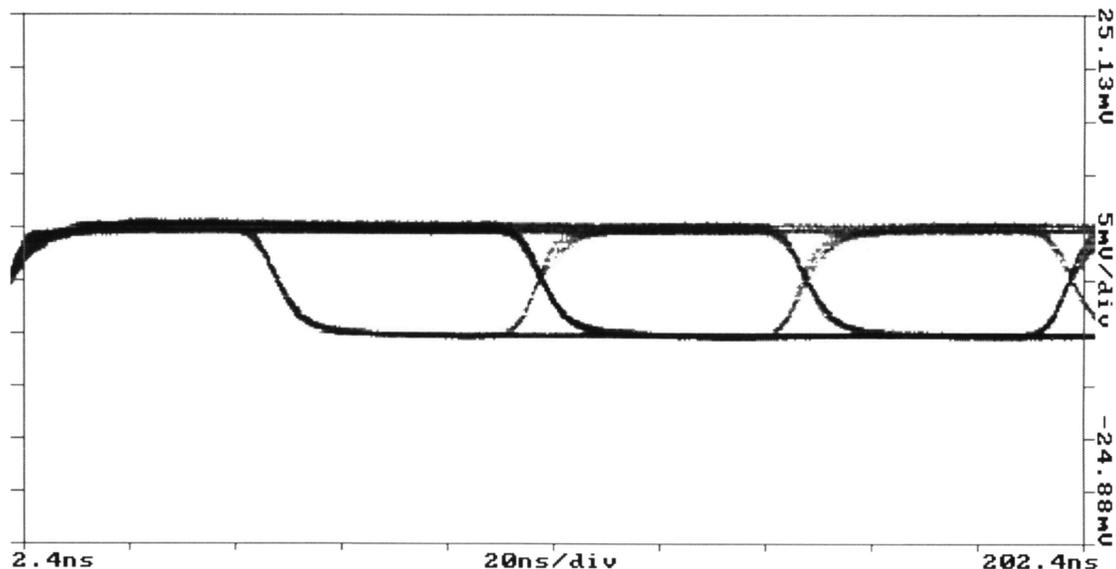
Fig. 17. Eye diagram of a switch output. The input was a laser modulated at 20 MHZ by use of an acousto-optic cell.

Table 3. Performance Estimates for a Scalable Switch ($N \geq 1024$ Channels) and Best Experimental Results to Date for 1×2, 2×2, and 4×4 BCGH Switches

Performance Estimates	Experimental Results
$\eta = 98\%$	$\eta \approx 60\%$ (four-level phase)
$R_g = R_m = 99\%$	$R_g = R_m \approx 99\%$
$C = 98\%$	$C = 98\%$
2×2 switch efficiency of 98% insertion loss of -0.64 dB	2×2 switch efficiency of $\approx 36\%$ insertion loss of -4 dB
2×2 switch SNR of 20–30 dB	1×2 switch SNR of 22 db (160:1)
	2×2 switch SNR of 16 dB (40:1)
	4×4 switch SNR of 13 dB (20:1)

References

1. See, for instance, IEEE J. Lightwave Technol., vol. 11, nos. 5 and 6, (1993).
2. F. Heismann, A. F. Ambrose, To. O. Murphy, and M. S. Whalen, "Polarization independent photonic switching system using fast automatic polarization controllers," IEEE Photon. Technol. Lett. **5,** 1341–1143 (1993).
3. G. A. De Biase, "Optical multistage interconnection networks for large-scale multiprocessor systems," Appl. Opt. **27,** 2017–2021 (1988).
4. K. M. Johnson, M. R. Surette, and J. Shamir, "Optical interconnection network using polarization-based ferroelectric liquid crystal gates," Appl. Opt. **27,** 1727–1733 (1988).
5. T. Nishi, T. Yamamoto, and S. Kuronagi, "A polarization-controlled free-space photonic switch based on a PI-LOSS switch," IEEE Photon. Technol. Lett. **5,** (1993).
6. K. Noguchi, T. Sakano, and T. Matsumoto, "A rearrangeable multi-channel free-space optical switch based on multistage network configuration," IEEE J. Lightwave Technol. **9,** 1726–1732 (1991).
7. Y. Wu, L. Liu, and Z. Wang, "Modified gamma network and its optical implementation," Appl. Opt. **32,** 7194–7199 (1993).
8. T. Sakano, K. Kimura, K. Noguchi, and N. Naito, "256 × 256 turnover-type free-space multichannel optical switch based on polarization control using liquid-crystal spatial light modulators," Appl. Opt. **34,** 2581–2589 (1995).
9. R. K. Kostuk, M. Kato, and Y. T. Huang, "Polarization prop-erties of substrate mode holographic interconnects," Appl. Opt. **29,** 3848–3854 (1990).
10. Y.-T. Huang, "Polarization-selective volume holograms: general design," Appl. Opt. **33,** 2115–2120 (1995).
11. T. Todorov, L. Nikolava, and N. Tomova, "Polarization holography. 1: A new high-efficiency organic material with reversible photoinduced birefringence," Appl. Opt. **23,** 4309–4591 (1984).
12. Q. W. Song, M. C. Lee, P. J. Talbot, and E. Tam, "Optical switching with photorefractive polarization holograms," Opt. Lett. **16,** 1228–1230 (1991).
13. J. Hossfeld, D. Columbus, H. Sprave, T. Tschudi, and W. Dultz, "Polarizing computer-generated holograms," Opt. Eng. **32,** 1835–1837 (1993).
14. J. E. Ford, F. Xu, K. Urquhart, and Y. Fainman, "Polarization selective computer generated holograms," Opt. Lett. **18,** 456–458 (1992).
15. J. E. Ford, F. Xu, A. Krishnamoorthy, K. Urquhart, and Y. Fainman, "Polarization-selective computer generated holograms for optical multistage interconnection networks," in *Optical Computing*, Vol. 7 of OSA Technical Digest Series (Optical Society of America, Washington, D.C., 1993), pp. 258–261.
16. F. Xu, J. E. Ford, and Y. Fainman, "Polarization-selective computer-generated holograms: design, fabrication, and applications," Appl. Opt. **34,** 256–266 (1995).
17. N. Nieuborg, C. Van de Pooel, A. Kirk, H. Thienpont, and I. Veretennicoff, "Polarization-selective diffractive and computer-

generated optical elements," in *Optical Computing*, Vol. 10 of OSA Technical Digest Series (Optical Society of America, Washington, D.C., 1995), pp. 124–126.

18. F. Xu, R. Tyan, P. C. Sun, Y. Fainman, C. Cheng, and A. Scherer, "Form birefringence of periodic dielectric nanostructures," Opt. Lett. **20,** 2457–2459 (1995).

19. G. Bromwell and J. Heath, "Classification categories and historical development of circuit switching topologies," Comput. Sur. **15,** (1983).

20. T. J. Cloonan, G. W. Richards, F. B. McCormick, and A. Lentine, "Architectural considerations for an optical extended generalized shuffle network based on 2-modules," in *Photonic Switching*, H. S. Hinton and J. W. Goodman, eds., Vol. 8 of OSA Proceedings Series (Optical Society of America, Washington, D.C., 1991), pp. 154–157.

21. A. V. Krishnamoorthy, P. Marchand, F. Kiamilev, and S. Esener, "Grain-size considerations for optoelectronic multistage interconnection networks," Appl. Opt. **31,** 5480–5507 (1992).

22. G. J. Swanson, "Binary optics technology: theory and design of multi-level diffractive elements," DARPA Tech. Rep. 854 (Defense Advanced Research Projects Agency, Washington, D.C., 1989).

23. L. Bhuyan and D. Agrawal, "Generalized shuffle networks," IEEE Trans. Comput. **C-32,** 1081–1090 (1983).

24. A. V. Krishnamoorthy and F. Kiamilev "Fanout, replication, and buffer-sizing for a class of self-routing packet-switched multistage photonic switch fabrics," in *Photonic Switching*, H. S. Hinton and J. W. Goodman, eds., Vol. 8 of OSA Proceedings Series (Optical Society of America, Washington, D.C., 1991), pp. 87–89. March 1995.

25. A. V. Krishnamoorthy, "3-dimensional optoelectronic N, M, F networks for neurocomputing and parallel processing," Ph.D. dissertation (University of California, San Diego, San Diego, Calif., 1993).

26. R. A. Spanke, "Architectures for large non-blocking optical space switches," IEEE J. Quantum Electron. **22,** 964–967 (1986).

27. T. J. Cloonan, F. McCormick, and A. Lentine, "Control injection schemes for photonic switching architectures," in *Photonic Switching*, H. S. Hinton and J. W. Goodman, eds., Vol. 8 of OSA Proceedings Series (Optical Society of America, Washington, D.C., 1991), pp. 162–165.

28. R. A. Spanke and V. Benes, "*N*-stage planar optical permutation network," Appl. Opt. **27,** 1226–1229 (1987).

29. V. E. Benes, "Growth, complexity and performance of telephone connecting networks," Bell Sys. Tech. J. **62,** 499–539 (1983).

30. K. Padmanaphan and A. Netraveli, "Dilated networks for photonic switching," IEEE Trans. Commun. **30,** 1357–1365 (1987).

31. S. C. Knauer, A. Huang, and J. H. O'Neill, "Self-routing switching network," in *CMOS VLSI Design*, N. Weste and K. Eshraghian, eds. (Addison-Wesley, Reading, Mass., 1988), Chap. 9, pp. 424–448.

32. N. K. Ailawadi, "Photonic switching architectures and their comparison," in *Frontiers in Computing Systems Research*, S. Tewksbury, ed. (Plenum, New York, 1990), Vol. 1, pp. 129–186.

33. A. V. Krishnamoorthy, F. Xu, J. Ford, and Y. Fainman, "Polarization-controlled multistage interconnection network based on birefringent computer generated holograms," in *Photonics for Processors, Neural Networks, and Memories*, J. L. Horner, B. Javidi, S. T. Knowel, and W. J. Miceli, eds., Proc. SPIE **2297,** 345–349 (1994).